



A study on the improvement of the cam phase control performance of an electric continuous variable valve timing system using a cycloid reducer and BLDC motor

SangWook Lee¹ · Soo-Whang Baek¹

Received: 6 November 2018 / Accepted: 20 March 2019 / Published online: 28 March 2019
© Springer-Verlag GmbH Germany, part of Springer Nature 2019

Abstract

This paper discusses the control performance improvement for an electric-continuous variable valve timing (E-CVVT) system using a brushless direct current (BLDC) motor and cycloid reducer. Each component of the E-CVVT system was implemented with mathematical analysis, and the response performance of the E-CVVT system was determined based on the mathematical model of the cam shaft motion, cam profile, cycloid reducer, BLDC motor, and controller. To control the intake valve timing of the engine, a cycloid speed reducer with a high reduction ratio capable of amplifying the output torque of a small BLDC motor was implemented. The change in valve speed due to the rotation of the cam shaft was represented by the curves described by the vertical movement of the valve using the cam profile. A control performance test apparatus was constructed and the torque of the intake cam shaft was measured and applied to the analysis so that the phase of the cam shaft could be changed using the E-CVVT system. To analyze the operating characteristics of the E-CVVT system, the BLDC motors were modeled using Simulink. The E-CVVT system controls the phase angle of the intake cam shaft. When the E-CVVT system sets the target phase angle, the motor controller generates the optimal motor speed command. The intake cam phase response speed depends on the setting of each PID parameter that changes the phase of the cam shaft. Through analysis and vehicle-based experiments, we confirmed the improvement of the E-CVVT system response performance according to the change of the PID parameter.

1 Introduction

Recently, the automobile industry has been attempting to improve fuel efficiency and reduce exhaust gas. In addition, many countries are strengthening regulations on automobile emissions because of concerns associated with environmental protection and public health, focusing on the reduction of carbon and nitrogen oxide emissions through the development of hybrid and electric vehicles (Böttcher and Müller 2015; Onat et al. 2015). Therefore, technologies for improving fuel economy, reducing the exhaust gas, and increasing the output of the internal combustion engine are attracting attention, and advanced automotive engine

electronic control techniques are being studied to achieve this (Cheng et al. 2016; Ashok et al. 2017).

Among the many advanced automotive engine electronic control technologies, the most noteworthy is variable valve control technology, which improves output and fuel efficiency by increasing intake and exhaust efficiency in the low and high speed rotation range of the engine (Grohn and Wolf 1989; Schäfer and Balko 2007). The opening and closing timing of the intake and exhaust valves and the valve overlap greatly affect the performance of the engine; as such, properly controlling the size of the valve overlap according to operating conditions can improve the performance of the vehicle. variable valve timing (VVT), variable valve lift (VVL), and variable valve event and lift (VEL) are examples of valve control technologies for this purpose. VVT is a technology that can improve engine performance in terms of fuel consumption, output improvement, and exhaust gas reduction throughout the full speed range by changing the timing of valve opening and closing, which were fixed according to factors such as the shape of the cam, in accordance with the engine speed

✉ Soo-Whang Baek
swbaek@honam.ac.kr

¹ Department of Automotive Engineering, Honam University,
417 Eodeung-daero, Gwangsan-gu, Gwangju 62399,
South Korea

and load (Hattori et al. 2008; Fujita et al. 2008). In contrast, VVL and VEL can increase the efficiency and performance of the engine by increasing the amount of intake air as the rotation speed of the engine is increased by adjusting the opening height of the valve. This study focuses specifically upon VVT technology.

VVT devices can be divided into three types according to the method by which valve closure timing is controlled: mechanical, electric, and hydraulic. Among them, hydraulic VVT is most commonly used within vehicles. In recent years, there has been an increase in the use of electric-continuous variable valve timing (E-CVVT) in response to the disadvantages of hydraulic VVT, which include a narrow operating range and slow response speed at low temperatures (Tsuchiya et al. 2009; Dixon 2012). When E-CVVT is applied, fuel consumption in idle state is improved by about 4%, while smoke is reduced by about 20%, and torque is increased by about 10% under low speed and high speed operation conditions (Hara et al. 2009). The E-CVVT consists of a mechanical reducer and an electric motor, which continuously controls valve timing. Due to design constraints, which are associated with the nature of vehicles and impact reliability, the reducer used in E-CVVT is small in volume and mass, and requires high precision and high torque performance specifications. Spur and planetary gears with conventional involute teeth require large numbers of stages in order to achieve high gear ratios. As a result, there are a large number of parts, as well as increased volume and mass, which present a challenge in the application of E-CVVT. To overcome this problem, a cycloid reducer is used within the E-CVVT system. In comparison with spur and planetary gears, the advantage of the cycloid reducer is that it induces rolling contact with a cycloid tooth type and has high efficiency and durability (Blagojevic et al. 2011). In order to drive the E-CVVT system, a motor is primarily used as an actuator. In comparison with conventional hydraulic CVVT systems, motor-driven E-CVVT systems provide higher combustion efficiency by precisely optimizing valve timing and improving operating range and response speed.

In this study, a brushless direct current (BLDC) motor with high output density and low inertia is used for the operation of an E-CVVT system. The BLDC motor is suitable for use in an automobile engine part because it has no brush structure and therefore does not generate sparks in the rectification process. In previous studies, an optimal design was implemented to improve the efficiency and maximum torque performance of BLDC motors (Baek 2018). In addition, in order to improve the control response performance of the E-CVVT system, it is necessary to consider control characteristics. However, there is insufficient research on the control performance verification of E-CVVT systems. This research examines the

mathematical analysis and control performance of E-CVVT systems using cycloid reducers and BLDC motors. Further, the features of the motor, the cycloid reducer, and the controller constituting the E-CVVT system are described. The kinetic energy and the potential energy were derived using the Lagrange equation in order to consider the motion of the valve. The overall torque due to the rotation of the servo motor and the rotational acceleration of the cam shaft were analyzed in consideration of the Rayleigh function and the total work generated by the servo motor. The shape of the cam is an important parameter to determine valve opening and closing. Therefore, the modeling of the valve was carried out in consideration of the shape of the cam. The torque of the cam shaft was measured by the engine and applied to the analysis. Additionally, we used Simulink to analyze the operating characteristics of the E-CVVT system. The E-CVVT control performance test apparatus was constructed and the relative phase change of the cam shaft was experimentally confirmed by driving the servo motor. The purpose of the E-CVVT system is to control the cam shaft phase according to the driving conditions of the vehicle. The response of the cam shaft depends on the control parameters. Therefore, the parameter of the PID controller suitable for the E-CVVT system was set and the improvement of the response characteristic was confirmed. The Simulink modeling of the E-CVVT system was used to confirm the change in the control response according to the variation of the PID control gain. As a result, we analyzed the response characteristics when the target value of the cam phase angle was set to 25° with 1000 rpm (cam shaft rotation).

It was observed that the improved control parameters were applied 0.1 s earlier than the initial value. The control performance test system of the variable valve system used motors of two different sizes to drive the cam shaft (3 kW-class servo motor) and the phase variable part (110 W-class BLDC motor), and to measure the torque and the rotation speed of each servo motor so that the control performance can be easily grasped. The two-stage cycloid reducer was used as the speed-reducing device of the phase varying part, and the timing chain was used for driving the cam shaft. Finally, a vehicle test was performed to confirm the E-CVVT control performance improvement. As a result of checking the characteristics of the intake valve displacement at a cam shaft rotation speed of 1000 rpm, the response characteristic of cam phase was shortened.

2 E-CVVT system

The E-CVVT system is shown in Fig. 1, and consists of an E-CVVT controller, servo motor, BLDC motor, motor control unit, and cylinder head block (Baek 2018). The

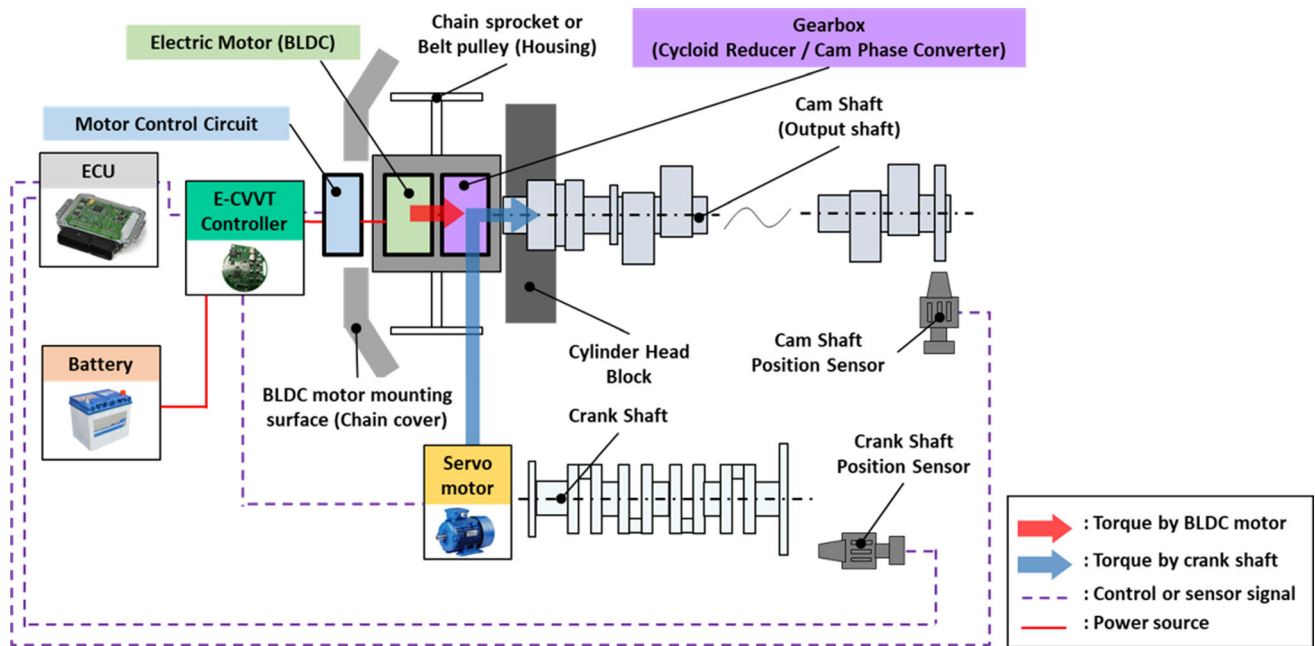


Fig. 1 Configuration of E-CVVT system

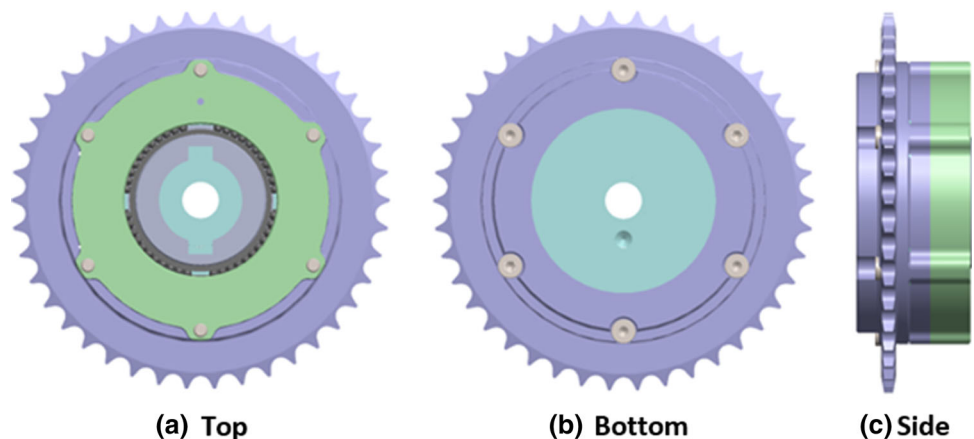
phase variable part consists of a BLDC motor and a two-stage cycloid reducer. The BLDC motor rotates to adjust the phase of the cam shaft through the cycloid reducer. The cylinder head block includes a cam shaft and a cam position sensor, and it is possible to measure the phase change between the cam shafts by the speed control of the BLDC motor. The cam shaft is connected to the medium servo motor of the drive by a chain and rotates at a constant speed. The speed of the servo motor measures the cam phase and controls the valve opening and closing time by feedback control to the E-CVVT controller.

2.1 Cycloid reducer

The E-CVVT system in this research uses a two-stage cycloid reducer, shown in Fig. 2. Cycloid reducers have the

advantage of achieving a large reduction ratio, while maintaining a small size in comparison to spur gears and planetary gears (White et al. 2013; Duan et al. 2017). The cycloid gearbox applied to the E-CVVT consists of a sprocket for driving the cam shaft, which is connected to the crankshaft, and a chain, a two-stage cycloid disk, an outer gear housing, an input eccentric shaft, and an output shaft. The cycloid disk and the pin-roller come into contact at various points and the load is dispersed in order to achieve high rigidity, good impact resistance, durability, and high efficiency. The deceleration in the cycloid reducer is shared by the first-stage and second-stage decelerator with one input eccentric shaft. The fixed outer gear housing and the output shaft, made up of pins, are brought into contact with the cycloid tooth profile.

Fig. 2 Cycloid reducer



Equation (1) represents the first-stage cycloid reduction ratio. The speed ratio of the first-stage cycloid is calculated as shown in Eq. (1), since the rotational speed of the outer gear is zero. The reason why the value of Eq. (1) has a negative sign is that the input shaft and the output shaft rotate in opposite directions.

$$N_2 = -\frac{N_1}{Z_1} \quad (1)$$

where N_1 is the speed of input shaft, N_2 is the speed of cycloid disc, and Z_1 is first-stage cycloid reduction ratio.

Equation (2) represents the second-stage cycloid reduction ratio. It is calculated using Eq. (2) by substituting Eq. (1).

$$Z_2 = -\frac{N_3 - N_1}{N_3 - N_2} = -\frac{N_3 - N_1}{N_3 - \left(-\frac{N_1}{Z_1}\right)} \quad (2)$$

where Z_2 is second-stage cycloid reduction ratio, N_3 is the speed of output flange with outer pins.

Using the Eqs. (1) and (2), the reduction ratio output by the cycloidal speed reducer can be obtained as shown in Eq. (3).

$$\frac{N_1}{N_3} = -\frac{Z_1(Z_2 + 1)}{Z_1 - Z_2} \quad (3)$$

The cycloid reducer can achieve a large reduction ratio due to the product of the number of teeth of the first-stage and the second-stage reducer, and the rotation direction of the input and output is the same. In addition, a larger reduction ratio can be obtained by reducing the difference in the number of teeth in the first- and second-stage reducers.

The reducer used in the E-CVVT system must take the engine layout into consideration, making it necessary to reduce the size and high reduction ratio. As mentioned earlier, the torque produced by the BLDC motor is transmitted to the cam shaft via a cycloid gear, the structure of which is shown in Fig. 3. The reduction ratio of the cycloid reducer was designed to be 100:1 in consideration of the torque magnitude and response speed required by the E-CVVT system. Table 1 shows the specifications of the cycloid reducer.

2.2 BLDC motor

In this study, we used an IPM-type BLDC motor to drive the E-CVVT system. This motor is suitable as a motor for automotive powertrains because it has a small size, high output, and good durability (Elakkia et al. 2015). The output power of the BLDC motor is expressed as Eq. (4), and the torque of the BLDC motor is expressed by Eq. (5),

considering the output power and the angular speed of the rotor.

$$P_e = e_a i_a + e_b i_b + e_c i_c \quad (4)$$

$$T_e = \frac{P_e}{\omega_m} = \frac{e_a i_a + e_b i_b + e_c i_c}{\omega_m} = k_T I \quad (5)$$

where P_e is output power, ω_m is the angular velocity of the rotor, k_T is the torque constant, I is the current of winding and e is the back-EMF of each phase of abc.

In order to calculate the characteristics of the BLDC motor, the IPM-type BLDC motor was modelled using Matlab/Simulink. As a simplified representation, the equivalent circuit of the BLDC motor is shown in Fig. 4.

The equation of motion of the BLDC motor is shown in Eq. (6).

$$T_e = T_L + J \frac{d\omega_m}{dt} + B\omega_m \quad (6)$$

where T_L is the load torque, J is the moment of inertia, and B is the coefficient of friction.

Figure 5 shows the structure of a BLDC motor, separated into the motor and controller components. In order to construct a controller in the BLDC motor, it is necessary to reduce the mechanical dimension, and a minimum circuit design has been performed for this purpose. The power part of the controller consists of a Pi filter and a reverse voltage protection circuit. The control unit consists of Freescale's S12ZVMC MCU (μ -control unit) and hall sensor interface. The drive part is composed of a three-phase symmetrical half-wave bridge circuit, two shunt resistors, and an MCU integrated with a regulator and gate driver in consideration of spatial restrictions. Table 2 shows the specifications of the BLDC motor controller.

2.3 Dynamic analysis considering valve motion

The motion of the valve is represented by a Lagrange equation that considers kinetic energy, position energy, and the Rayleigh dissipation function (Incerti 2006). When the rotational angle of the cam shaft is α , the motion of the valve is expressed as (7).

$$\frac{\delta W}{\delta \alpha} = \frac{d}{dt} \left(\frac{\partial T}{\partial \dot{\alpha}} \right) - \frac{\partial T}{\partial \alpha} + \frac{\partial R}{\partial \dot{\alpha}} + \frac{\partial V}{\partial \alpha} \quad (7)$$

where T is the kinetic energy of the system, V is the potential energy of the system, R is the Rayleigh dissipation function, and W is the work performed by a non-conservative action.

In this case, assuming that the valve moving along the cam shaft is composed of masses M_1 and M_2 , when the angle of rotation of the cam shaft is defined as a function of the angle of rotation α , as shown in Eq. (8), the displacement y of mass M_1 as shown in Eq. (9).

Fig. 3 Structure of cycloid reducer

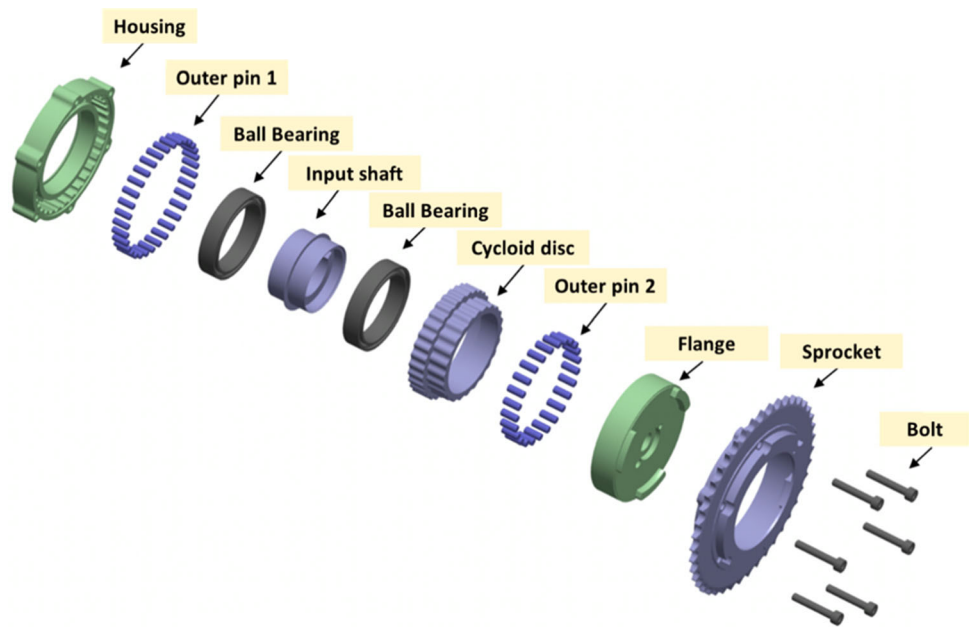


Table 1 Specification of cycloid reducer

Items	Value	Unit
Gear ratio	100:1	–
Minimum of input torque	0.8	Nm
Maximum of output torque	20	Nm
Maximum of phase shift angle	45	°

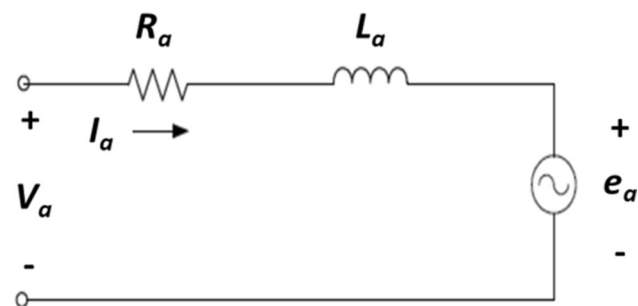


Fig. 4 Equivalent circuit of the BLDC motor

$$y = y(x) \tag{8}$$

$$\dot{y} = \dot{y}(x)\dot{x} \tag{9}$$

The kinetic energy T is expressed as the following Eq. (10), taking into account the moment of inertia J_m of

the motor and the moment of inertia J_c of the cam shaft as a product of mass and velocity.

$$T = \frac{1}{2}(J_m\dot{\phi}^2 + J_c\dot{\alpha}^2 + M_1\dot{y}^2 + M_2\dot{x}^2) \tag{10}$$

The potential energy V is expressed by the following Eq. (11), taking into consideration the spring constants k_1 and k_2 for the masses M_1 and M_2 , constituting the valve and the deflections of the springs due to static loads η_1 and η_2 .

$$V = \frac{1}{2}\{k_1(y - x + \eta_1)^2 + k_2(x + \eta_2)^2\} \tag{11}$$

The damping energy by the Rayleigh function is given by the following Eq. (12), considering the damping coefficients c_1 and c_2 of each mass constituting the valve.

$$R = \frac{1}{2}\{c_1(\dot{y} - \dot{x})^2 + c_2\dot{x}^2\} \tag{12}$$

Kinetic energy in Eq. (10), potential energy in Eq. (11), and damping energy in Eq. (12) are summarized using Eq. (7). As a result, the total torque due to the rotation of the servo motor and the rotational acceleration of the cam shaft can be summarized by two differential equations, as shown in Eq. (13).

$$\begin{cases} T_{total} = T_m - T_r = (J_c + J_m + M_1y'^2)\ddot{\alpha} + M_1y'y''\alpha^2 + k_1y''(y - x + \eta) + c_1y'(y'\dot{\alpha} - \dot{x}) \\ \ddot{x} = \frac{1}{M_2}\{-(k_1 + k_2)x + k_1y - (c_1 + c_2)\dot{x} + c_1y'\dot{\alpha}\} \end{cases} \tag{13}$$

Fig. 5 Structure of the BLDC motor

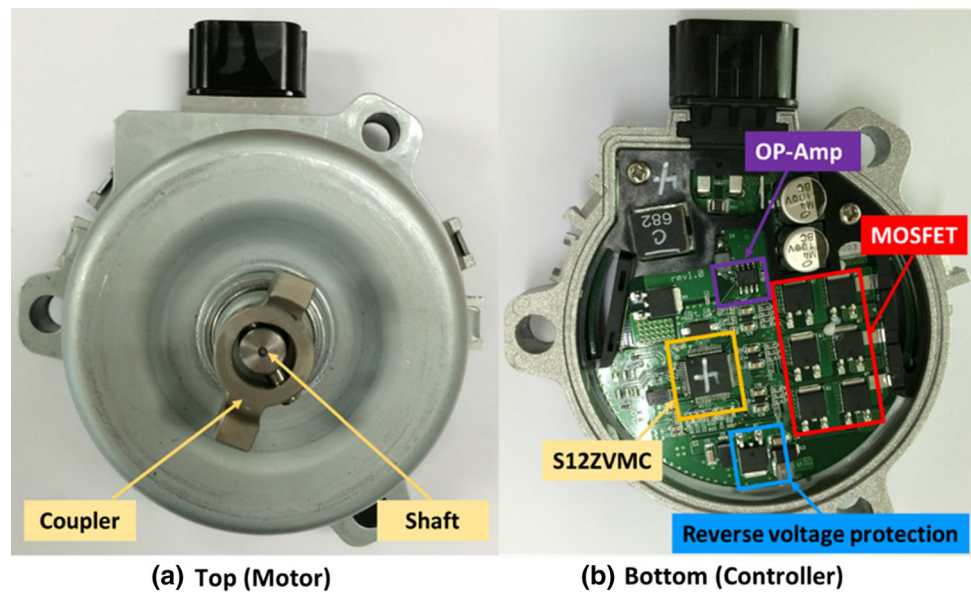


Table 2 Specification of the BLDC motor controller

Items	Value			Unit
	Minimum	Typical	Maximum	
Power part				
Input voltage	–	12	–	V
Over-voltage protection	16.5	–	–	V
Under-voltage protection	–	–	6.75	V
Operating temperature range	– 40	–	150	°C
Control part				
Speed control output accuracy	– 200	0	200	rpm
Cam phase angle accuracy	– 1	0	1	°
Cam phase angle overshoot	– 1	0	1	°
Drive part				
PWM duty range	5	–	95	%
Maximum of current condition	–	–	30	A_{rms}
Speed range of BLDC motor	100	–	8000	rpm

where J_c is the cam moment of inertia, J_m is the engine moment of inertia, T_m is the torque of the BLDC motor, T_r is resistant torque, x is the displacement of the 1st mass in the valve system and y is the displacement of the 2nd mass in the valve system.

2.4 Valve modeling considering cam shape

The valve repeatedly opens and closes due to the rotation of the cam, which has an irregular shape. The shape of the cam varies according to the purpose of use, while the speed with which the valve opens and closes depends on the shape. The vertical profile of the valve in relation to the cam surface while the cam shaft rotates is called a cam profile (Incerti 2011). Generally, it is a cam curve for

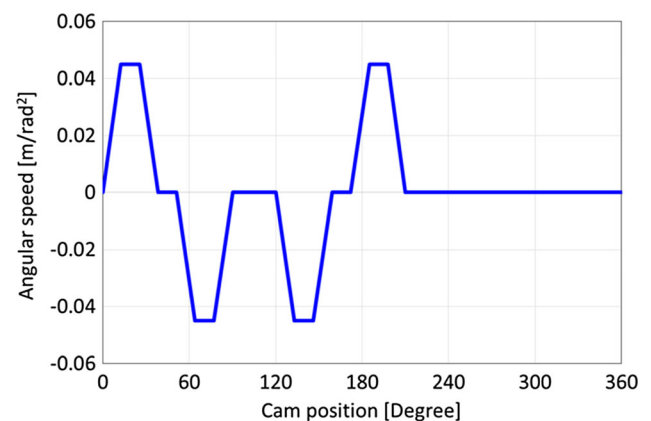


Fig. 6 Cam profile

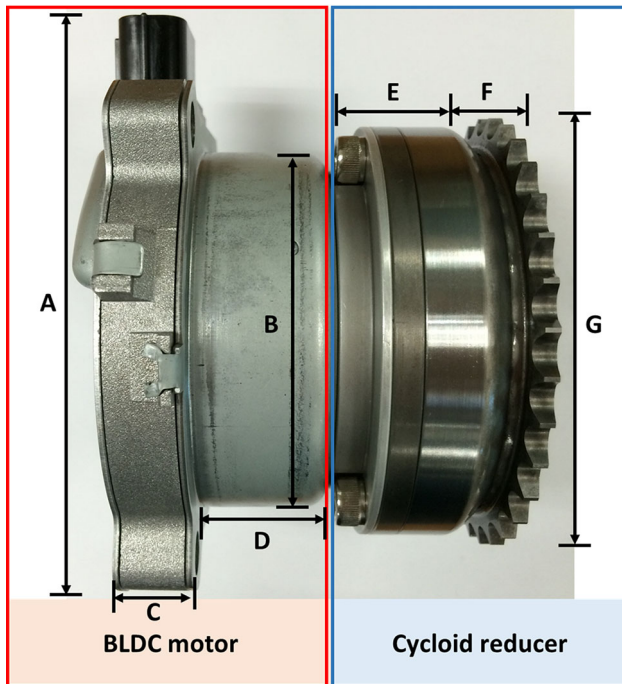


Fig. 7 Combination of BLDC motor and cycloid reducer

Table 3 Dimensions of BLDC motor and cycloid reducer

	Values	Unit
Items		
BLDC motor	130	mm
Outer diameter of motor (B)	80	mm
Length of controller (C)	20	mm
Length of motor (D)	50	mm
Cycloid reducer		
Length of housing (E)	30	mm
Length of sprocket (F)	15	mm
Outer diameter of sprocket (G)	92	mm

simple motion expression, and it is expressed by a mathematical model such as a trapezoid, a cycloid, a single harmonic function, and a polynomial curve. However, high-order polynomials and high-harmonic components are used for the cam curve to consider the high-speed rotation of the automobile engine (Jelenschi et al. 2011). In this paper, the velocity change of the valve is expressed using the polynomial shape curve in Fig. 6.

Using the assembled BLDC motor and cycloid reducer shown in Fig. 7, the torque of the intake cam shaft was measured. The coupler located on the shaft of the BLDC motor is coupled to the input shaft of the cycloid reducer and rotates the cycloid reducer through the operation of the BLDC motor. The dimensions of the BLDC motor and the cycloid reducer are shown in Table 3.

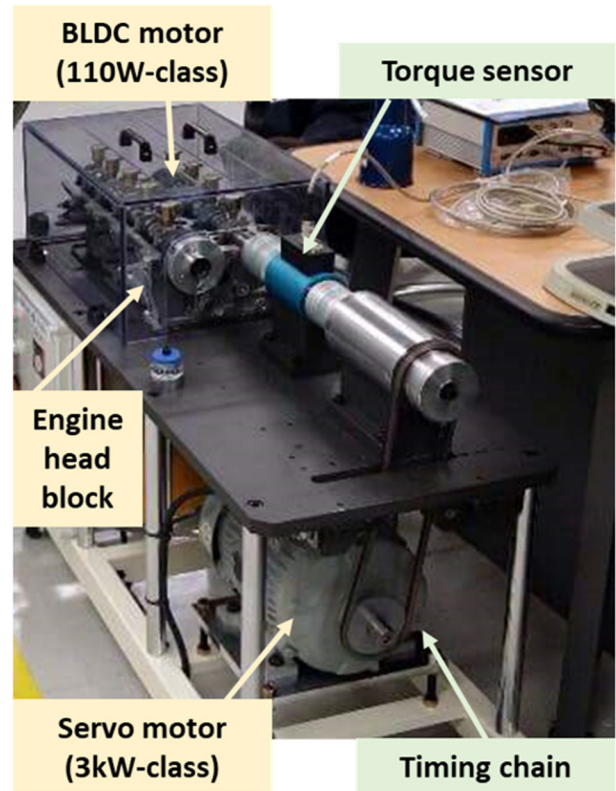


Fig. 8 Configuration of control performance test apparatus

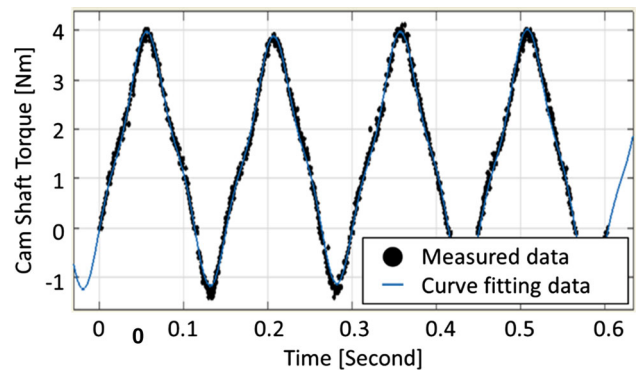


Fig. 9 Cam shaft torque at 1000 rpm (curve fitting)

To drive the E-CVVT system, the torque value of the intake shaft of the engine must be known. This is because the E-CVVT system can be controlled only when the cycloid reducer generates an output torque greater than the torque of the input shaft of the engine. Therefore, to measure the torque value of the intake shaft of the engine, the control performance test apparatus of the E-CVVT system was used, shown in Fig. 8. The control performance test system consists of a servo motor, a BLDC motor (5 kW and 110 W-class), an engine head block including a cam shaft, a timing chain, and a torque sensor. The 5 kW-class servo motor serves as the crank shaft of the actual

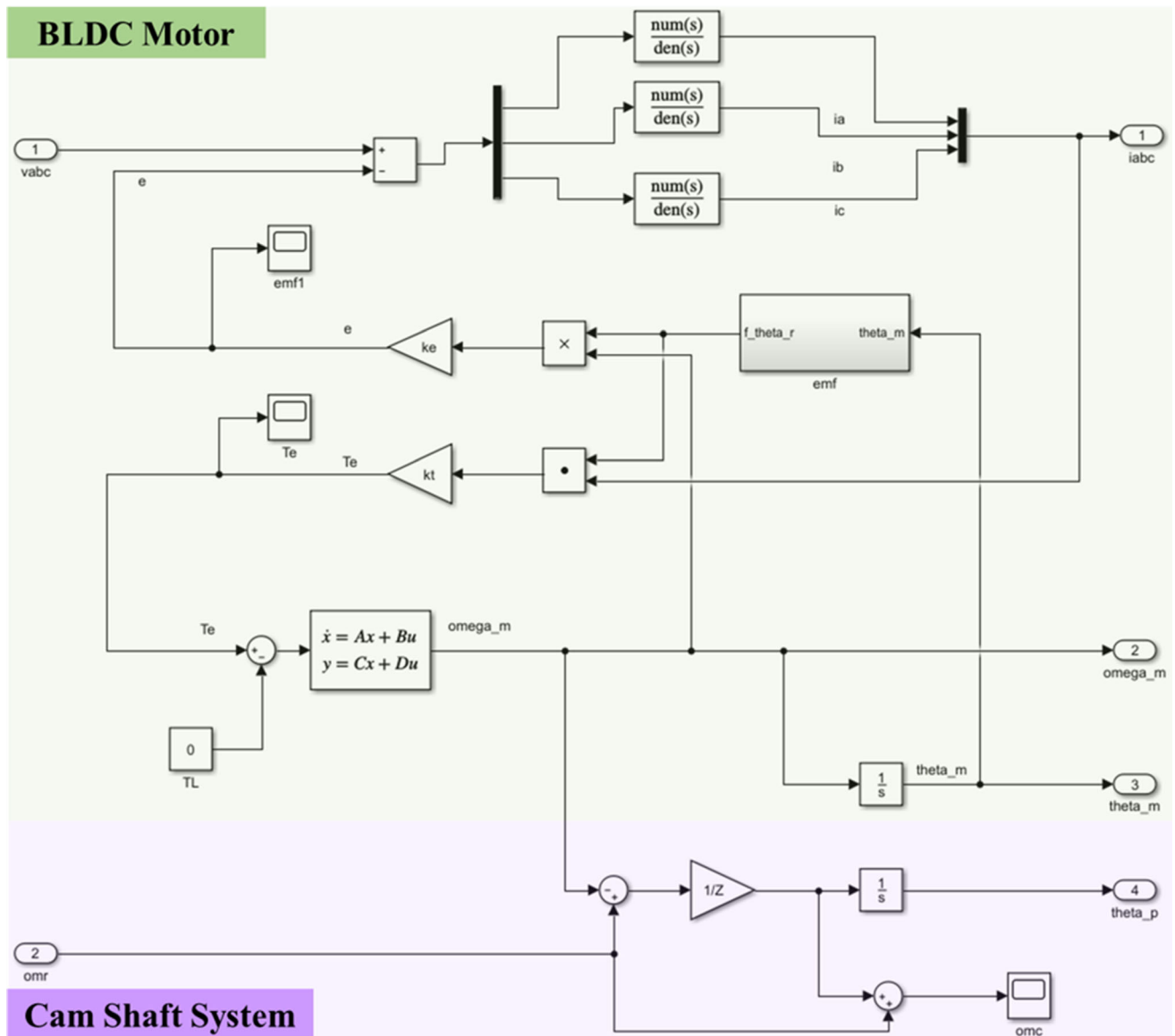


Fig. 12 BLDC motor and cam shaft system (using Simulink)

speed command that takes the actual rotational speed of the cam shaft into account. In order to transfer the command value calculated by the PID controllers to the BLDC motor driver, the control conversion block is constructed in order to convert the command value component into magnitude and direction. Here, since the magnitude of the command must be converted into the PWM value, the PWM signal generation block is constructed. As a result, the BLDC motor rotates to change the phase of the cam shaft according to the setting of the PID parameter.

Figure 12 shows the BLDC motor and cam shaft system using the Simulink. The BLDC motor part calculates the characteristics of the three-phase winding current and the output torque of the motor, while the cam shaft system part

analyzes the cam phase change in relation to the rotation of the BLDC motor.

Simulink modeling of the E-CVVT system was used to confirm the change in the control response according to the variation of the PID control gain. As shown in Fig. 13, the control response characteristics according to the variation of the control speed controller and the position controller parameter gain were confirmed. Simulation tests were performed by setting the cam shaft to rotate constantly at 1000 rpm, inputting the target phase of 25°, and changing the gains of the PID control parameters of the position controller and the motor speed controller. If an overshoot occurred in the cam phase angle change characteristic when controlling the E-CVVT system, it would impact the cycloid reducer and the BLDC motor, which would

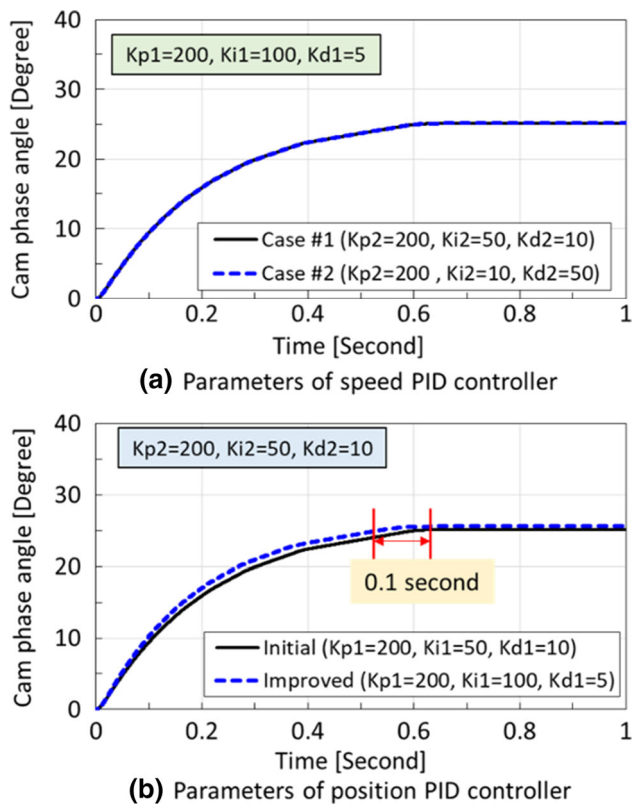


Fig. 13 Comparison of response characteristic at 1000 rpm (by simulation)

adversely affect the durability of the system. Therefore, it is important to control the cam phase to prevent overshoot when the phase of the cam shaft is changed to ensure mechanical protection of the cycloid reducer and the BLDC motor. Figure 13a shows two cases in which the response speed change is small as a result of changing the gain of the PID control parameter of the speed controller, while the control gain of the position controller is fixed. Figure 13b shows the difference in response speed as a result of changing the gain of the PID control parameter of the position controller and fixing the gain of the speed controller (case # 1: $K_{p2} = 200$, $K_{i2} = 50$, and $K_{d2} = 10$). When the gain of the PID control parameter of the position controller is changed to ($K_{p1} = 200$, $K_{i1} = 100$, and $K_{d1} = 5$), it can be seen that the improved parameter was applied 0.1 s earlier than the initial value.

4 Verification of experiment

Using the control performance test apparatus shown in Fig. 8 and described in the previous section, the speed of the servo motor and the speed of the BLDC motor were determined and are shown in Fig. 14. Thus, it was possible to determine the phase change of the cam shaft according

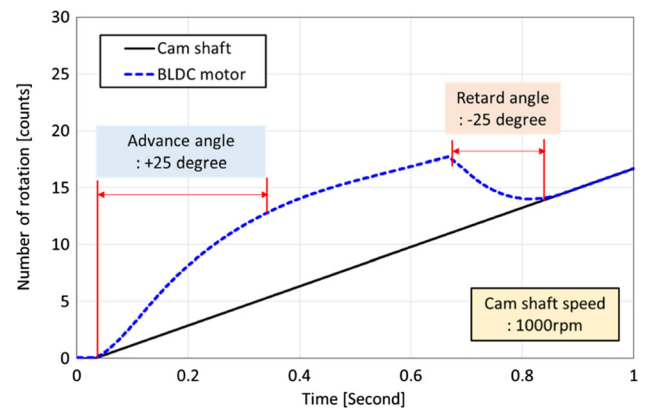
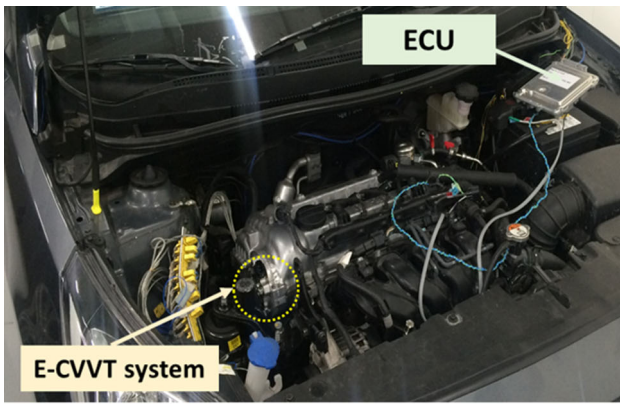


Fig. 14 Comparison of rotational speed characteristics between the BLDC motor and the cam shaft (by control performance test apparatus)

to the control input. The cycloid reducer and the cam shaft rotate in the same direction in the test apparatus, which imitated the same conditions as those of the car engine head block. When the advanced control of the cam phase angle was performed, it was necessary for the BLDC motor to rotate at a higher speed than the cam shaft speed in order to advance the cam phase. On the other hand, when the retard control of the cam phase angle was performed, the speed of the BLDC motor was controlled to be lower than the rotational speed of the cam shaft, or in the reverse direction. Therefore, the response speed of the retard condition was faster than that of the advanced condition.

Vehicle tests were conducted to verify the control performance of the E-CVVT system. Figure 15 shows a vehicle test setup. Specifically, Fig. 15a shows the vehicle mounting of the E-CVVT system, while Fig. 15b shows the data acquisition environment. The comparison object was characteristic of the valve displacement for the valve timing control. The vehicle test was performed with an engine rotation speed of 2000 rpm and a cam shaft speed of 1000 rpm, and the response characteristic data was acquired using the CAN communication. The vehicle test conditions are shown in Table 4.

Figure 16 shows the characteristic displacement of the valve and shows the opening and closing state of the valve. Specifically, Fig. 16a shows the valve opening/closing state of the cam shaft due to engine rotation, while Fig. 16b is an enlarged view of the phase change from 0.5 to 0.7 s. The control parameters described in Fig. 13 were applied to the E-CVVT system controller in order to compare the initial and improved characteristics. As the rotational speed of the BLDC motor increases under the advancing condition, the valve opens and closes at an earlier time. It can be seen that the phase of the cam shaft under the improved condition advanced faster than under the initial condition. In addition, it can be seen that the phase of the cam shaft



(a) Vehicle mounting of the E-CVVT system



(b) Data acquisition environment

Fig. 15 Vehicle test setup

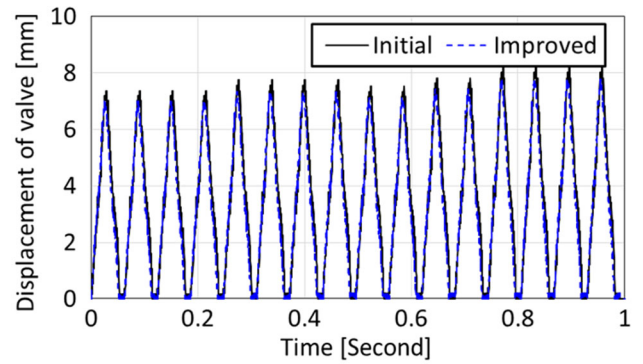
Table 4 Vehicle test condition

Items	Value	Unit
Input voltage	13.5	V
Current limit	25	A
Engine speed	2000	rpm
Cam shaft speed	1000	rpm
Variable range of cam phase angle	0–25	°
Ambient temperature	25	°C

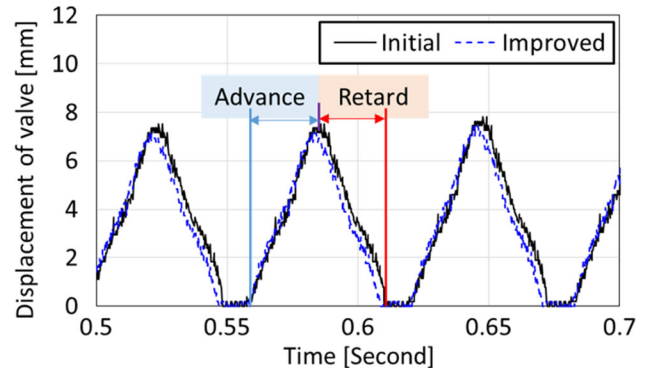
retarded as the rotation speed of the BLDC motor decreased in the retarding condition. It can be seen that the phase of the cam shaft of improved condition retarded faster than the initial condition. Finally, the improvement of the phase response characteristic of the cam shaft was verified through the vehicle test.

5 Conclusion

In this paper, we proposed a method to improve the PID control parameter of BLDC motors used in E-CVVT systems to improve the advancing and retarding response



(a) Displacement of valve (0 to 1 second)



(b) Enlarged (0.5 to 0.7 second)

Fig. 16 Characteristic of valve displacement (by vehicle test)

characteristics of intake valves. In addition, the Lagrange equation and Rayleigh dissipation function were described for the implementation of BLDC motor, controller of the BLDC motor, cycloid reducer, and mathematical analysis of the E-CVVT system. The control of the E-CVVT system was performed based on the PID control and the Simulink block was used for verification. It was confirmed that the response characteristic of the cam shaft phase did not have an overshoot so as not to apply a mechanical impact to the input shaft of the cycloid reducer, whose phase of the E-CVVT system changed, and the response speed of the E-CVVT system was improved. In addition, the vehicle test confirmed that the proposed control parameters are suitable for improving the performance of the E-CVVT system. The control method of the E-CVVT system developed in this study is expected to improve the response characteristics by simply determining the PID control parameters, as well as to improve vehicle fuel efficiency and output through application to the automotive motor system for the powertrain.

Acknowledgements This paper was supported by the National Research Foundation of Korea (NRF) Grant funded by the Korea government (MSIT) (no. 2017R1C1B5075525); This study is the result of a research carried out as a part of “Green Vehicle Component Cluster Project” supported by the Ministry of Trade, Industry

and Energy (MOTIE) and Korea Institute for Advancement of Technology (KIAT) (P0000760).

References

- Ashok B, Denis Ashok S, Ramesh Kumar C (2017) Trends and future perspectives of electronic throttle control system in a spark ignition engine. *Annu Rev Control* 44:97–115. <https://doi.org/10.1016/j.arcontrol.2017.05.002>
- Baek SW (2018) Optimum shape design of a BLDC motor for electric continuous variable valve timing system considering efficiency and torque characteristics. *Microsyst Technol* 24:4441–4452. <https://doi.org/10.1007/s00542-018-3991-2>
- Blagojevic M, Marjanovic N, Djordjevic Z, Stojanovic B, Disic A (2011) A new design of a two-stage cycloidal speed reducer. *ASME J Mech Des* 133(8):085001-7. <https://doi.org/10.1115/1.4004540>
- Böttcher CF, Müller M (2015) Drivers, practices and outcomes of low-carbon operations: approaches of German automotive suppliers to cutting carbon emissions. *Bus Strategy Environ* 24(6):477–498. <https://doi.org/10.1002/bse.1832>
- Cheng A, Li H, Xiong L (2016) A model-based calibration method of automotive electronic control unit. *Wuhan Univ J Nat Sci* 21(2):171–177. <https://doi.org/10.1007/s11859-016-1155-8>
- Dixon M (2012) Variable camshaft timing/variable valve timing. Presentations. Paper 29. http://opensiuc.lib.siu.edu/auto_pres/29. Accessed 5 Oct 2012
- Duan H et al (2017) Structure design and motion simulation of the pin-cycloid gear planetary reducer with ring-plate-type. *IOP Conf Ser Earth Environ Sci* 69:012183. <https://doi.org/10.1088/1755-1315/69/1/012183>
- Elakkia E et al (2015) Design and modeling of BLDC motor for automotive applications. *Int J Electr Electron Eng Telecommun* 1(1):42–48
- Fujita T, Onogawa K, Kiga S, Mae Y et al (2008) Development of innovative variable valve event and lift (VVEL) system. *SAE Tech Pap.* <https://doi.org/10.4271/2008-01-1349> (2008-01-1349)
- Grohn M, Wolf K (1989) Variable valve timing in the new Mercedes-Benz four-valve engines. *SAE Tech Pap.* <https://doi.org/10.4271/891990>
- Hara S, Suga S, Wateabe S, Nakamura M (2009) Variable valve actuation systems for environmentally friendly engines. *Hitachi Rev* 58(7):319–324
- Hattori M, Inoue T, Mashiki Z, Takenaka A et al (2008) Development of variable valve timing system controlled by electric motor. *SAE Int J Engines* 1(1):985–990. <https://doi.org/10.4271/2008-01-1358>
- Incerti G (2006) Dynamic modelling of cam indexers driven by DC servomotors. *IEEE Int Conf Control Appl* 2006:1392–1397. <https://doi.org/10.1109/CACSD-CCA-ISIC.2006.4776845>
- Incerti G (2011) Dynamic behaviour of elastic cam devices driven by servomotors with PID velocity control. *IEEE Int Conf Autom Sci Eng* 2011:268–273. <https://doi.org/10.1109/CASE.2011.6042401>
- Jelenschi L, Cofaru C, Sandu G, Aleonte M (2011) State of the art of engine valve and tappet rotation. *Bull Transilvania Univ Braşov Ser I* 4(53):19–24
- Onat NC, Kucukvar M, Tatari O (2015) Conventional, hybrid, plug-in hybrid or electric vehicles? State-based comparative carbon and energy footprint analysis in the United States. *Appl Energy* 150:36–49. <https://doi.org/10.1016/j.apenergy.2015.04.001>
- Schäfer J, Balko J (2007) High performance electric camshaft phasing system. *SAE Tech Pap.* <https://doi.org/10.4271/2007-01-1294> (2007-01-1294)
- Tsuchiya T, Hosoi H, Hoshi K, Shimamura H et al (2009) Newly developed inline 4 AR series SI engine. *SAE Tech Pap.* <https://doi.org/10.4271/2009-01-1048> (2009-01-1048)
- White A, Choi J, Zhu G (2013) Dynamic output-feedback gain-scheduling control of an electric variable valve timing system. *Am Control Conf (ACC)* 2013:3619–3624. <https://doi.org/10.1109/ACC.2011.5990625>

Publisher's Note Springer Nature remains neutral with regard to jurisdictional claims in published maps and institutional affiliations.